Front. Earth Sci. 2023, 17(1): 30–44
https://doi.org/10.1007/s11707-022-1031-0

RESEARCH ARTICLE

Characteristics and evolution of faults in the north-central Yin'e Basin and the effects on the coal-seam in the Cretaceous strata

Qiang YU[1], Baojiang WANG (✉)[2], Zhanli REN (✉)[3], Xianyao SUN[1], Xianghe LEI[1], Ahmed KHALED[1], Qike YANG[1]

1 School of Earth Science and Resources, Chang'an University, Xi'an 710054, China
2 School of Information Technology, Xichang University, Xichang 615013, China
3 Department of geology, Northwest University, Xi'an 710069, China

Abstract Research on the characteristics of faults and their evolutionary history since the Cretaceous in the Suhongtu-Dagu depressions can provide a theoretical basis for geological evaluation of the coal seams in the Suhongtu Formation in the northern-central region of the Yin'e Basin. Using 3-D seismic-logging inversion techniques, seismic stratigraphic calibration, stratigraphic sequence delineation, and thickness calculations on the Suhongtu-Dagu depressions were carried out to clarify the planar and profile distributions of the faults, as well as the evolutionary history of these faults and the tectonic history of the depressions. The results of this study revealed that the distribution of the faults in the Suhongtu-Dagu depressions in the northern part of the Yin'e Basin varies with region, and the fault system was multi-period, orthotropic, north-east-trending, and north-north-east-trending, with a certain degree of inheritance in terms of the geological setting. Three types of faults were identified: Y-shaped fractures, reverse Y-shaped fractures, and parallel fractures, which can be classified as Paleozoic-Cenozoic continuous syncline faults and intra-depression faults from the top of the Permian to the Upper Cretaceous series and inter-stratigraphic adjustment faults within the Cretaceous System, respectively. The evolution of these faults can be divided into three phases: the controlling faults were the faults that existed before the Early Cretaceous and had been active since then; synclinal faults that formed during the Early Cretaceous; and modified faults that formed since the Early Cretaceous. The development and modification of the coal seams in the Cretaceous Suhongtu Formation in the Hari, Kuanzihu, and Babei sags were strongly controlled and influenced by a multi-phase complex fault system.

Keywords coal-seam, tectonic evolution, seismotectonic interpretation, Hari depression, 3D distribution of faults, oil-gas exploration, Guaizihu depression

1 Introduction

Coal is an important part of coal-measure strata, and it is also one of the rock types with a high organic matter enrichment. Several sedimentary basins in northern China, including the Yin'e Basin, have a certain potential for the development of coal and related resources (Ren and Chen, 2020; Wu et al., 2020a). In the past, when analyzing the oil and gas resources in the Yin'e Basin, more attention was paid to the analysis of the Cretaceous argillaceous source rocks, but little attention was paid to the coal-measure source rocks because the oil and gas resources that have been discovered in this basin are mainly concentrated in the Cretaceous strata, and it was thought that the only source rock was the Cretaceous organic-rich mudstone and no or very few coal-measure rocks participated in the hydrocarbon generation and expulsion process. In addition, in the process of oil and gas development and production, the drilling stops once the target interval is drilled, which has resulted in a lack of samples of and data on the multiple sets of sedimentary strata buried deeper, such as the Triassic to Carboniferous strata, and it has constrained our understanding of the deep coal measure strata in the Yin'e Basin.

In recent years, with the development of deep drilling and 3-D seismic work, people have discovered Carboniferous-Permian, Jurassic, and Cretaceous coal-measure

Received December 9, 2021; accepted October 10, 2022

E-mail: xcc20200168@xcc.edu.cn (Baojiang WANG)
renzhanl@nwu.edu.cn (Zhanli REN)

strata in the northern part of the Yin'e Basin (Wu et al., 2020b; Zhou et al., 2021), and it has been reported that in addition to the Lower Cretaceous semi-deep lacustrine-shallow lacustrine source rocks, coal-bearing source rocks with certain hydrocarbon-generating properties are also developed in this area. These rocks are swamp facies coal-bearing source rocks and were developed in a fluvial-lake system in an inland basin. In addition, they were mainly developed in the Middle-Lower Jurassic coal-measure strata in the fault depression period and the Lower Cretaceous Bayingobi Formation and Suhongtu Formation (Chen et al., 2001; Han et al., 2015; Qi et al., 2021; Chen et al., 2022; Xing et al., 2022) in the Juyanhai Depression, Dagu-Suhaitu Depression, and Shangdan Depression. The lithology consists of coal-bearing mudstone, carbonaceous mudstone, and coal. The Cretaceous argillaceous and Middle-Lower Jurassic coal-bearing strata constitute two sets of source rocks consisting of self-generating, self-storing, and reservoir-capping assemblages.

Several studies have shown a good relationship between tectonic evolutions and faults distributions (Wang et al., 2017; Fu et al., 2021; Li et al., 2021a, 2021b). Three-dimensional seismic inversion and logging-seismic combination techniques are used in this study to clarify the characteristics and distribution of the fault system. Furthermore, the evolutionary history of the fault system can be determined by combining palaeo-tectonic recovery techniques. Taking the Lower Cretaceous Suhongtu Formation where the coal seam was developed as the research object, the evolutionary history of faults within the Hari Sag, the Guaizihu Sag, and the Baibei Sag since the Cretaceous period were discussed by identifying the spatial distribution as well as planar and sectional characteristics of the faults through the tectonic interpretation of 3D seismic sections and drilling data. This work is an important guide to the characterization and evolution of the coal-bearing stratigraphy in the northern part of the Yin'e Basin.

2 Geologic settings

The Yingen-Ejinaqi Basin (Yin'e Basin) is located in the transition zone between the ancient Asian Ocean and the Tethys Ocean structures, and it is the complex transitional region between the China-Korea Craton, the Tarim Craton, the Tianshan-Xingan Orogen, and the Qinling-Qilian-Kunlun Orogen. It covers an area of 12.13×10^4 km^2 and consists of more than 20 small Mesozoic graben basins of different sizes, and it has a good potential for oil and gas exploration (Fig. 1).

Tectonic units of the Yin'e Basin can be divided into four uplifts, including the Lvyuan, Luotexitan, Zongnaishan and Chulu uplifts, and seven depressions, including the Juyanhai, Wutaohai, Dagu, Suhongtu, Suhaitu, Shangdan and Chagan depressions (Fig. 1). The research area of this study is located in the northern part of the Yin'e Basin, including the Guaizihu, Hari, Harinan, Babei, Banan and Wulan sags with a total area of 3.59×10^4 km^2 (Fig. 1).

The geological features on the two sides of the Altun-Tagh Fault are different (Yin et al., 2002; Yu et al., 2018). The Eugerwusu Fault, which is the northern boundary of the Naishanchulu Uplift (Fig. 1), separates the study area into a northern part with an epimetamorphism basement composed of Lower Paleozoic-Middle Devonian strata and a southern part with a metamorphic basement composed of Archean-Proterozoic strata (Wu et al., 2020b; Lu et al., 2018). The sedimentary formations in the Yin'e Basin include a basement composed of Lower Paleozoic and older strata. The Late Paleozoic strata are dominated by marine sediments, and the Mesozoic strata consist of continental sediments. In the study area, the Triassic and Jurassic systems are absent and the Paleozoic strata underlie the Cretaceous (Xiao et al., 2015), resulting in an unconformity (Table 1).

The lower part of the Carboniferous is composed of gray-green andesite, rhyolite intercalated with hard sandstone, feldspar sandstone, silty mudstone and thin limestone. The middle part of is composed of carbonate rock characterized by gray sand (gravel) clastic limestone, oolitic limestone, bioclastic limestone intercalated with calcareous sandstone and mudstone. The upper part is composed of multiple normal cycles of coarse lower (silty fine sandstone intercalated with thin limestone) and upper fine (dark mud shale), intercalated with thin limestone.

The Permian strata in the Hari Sag include the Maihanhada Formation in the Lower Permian, the Aqide Formation in the middle Permian and Haersuhai Formation in the upper Permian. The Permian strata are distributed relatively stable, with its lower lithology consisting of andesite and quartz andesite with brown and gray mudstone and tuff conglomerate. The middle section consists of brown mudstone and tuff conglomerate interbedded with volcanic rocks. The upper part is mainly composed of gray mudstone and argillaceous sandstone sandwiched with fine tuffaceous sandstone and volcanic rock. In contrast, the Permian System in the Babei Sag is mainly composed of fine clastic rocks. Its lower part is interbedded by gray mudstone, tuffaceous mudstone and tuffaceous sandstone, and the middle part is interbedded between mudstone and argillaceous sandstone (Table 2) (Chen et al., 2018; Chen et al., 2019b).

The Cretaceous strata can be divided into the Bayingebi Formation (K1b), the Suhongtu Formation (K1s) and the Yingen Formation (K1y) of the Lower Cretaceous, and the Wulansuhai Formaton (K2w) of the Upper Cretaceous.

The Quaternary strata are distributed in unequal

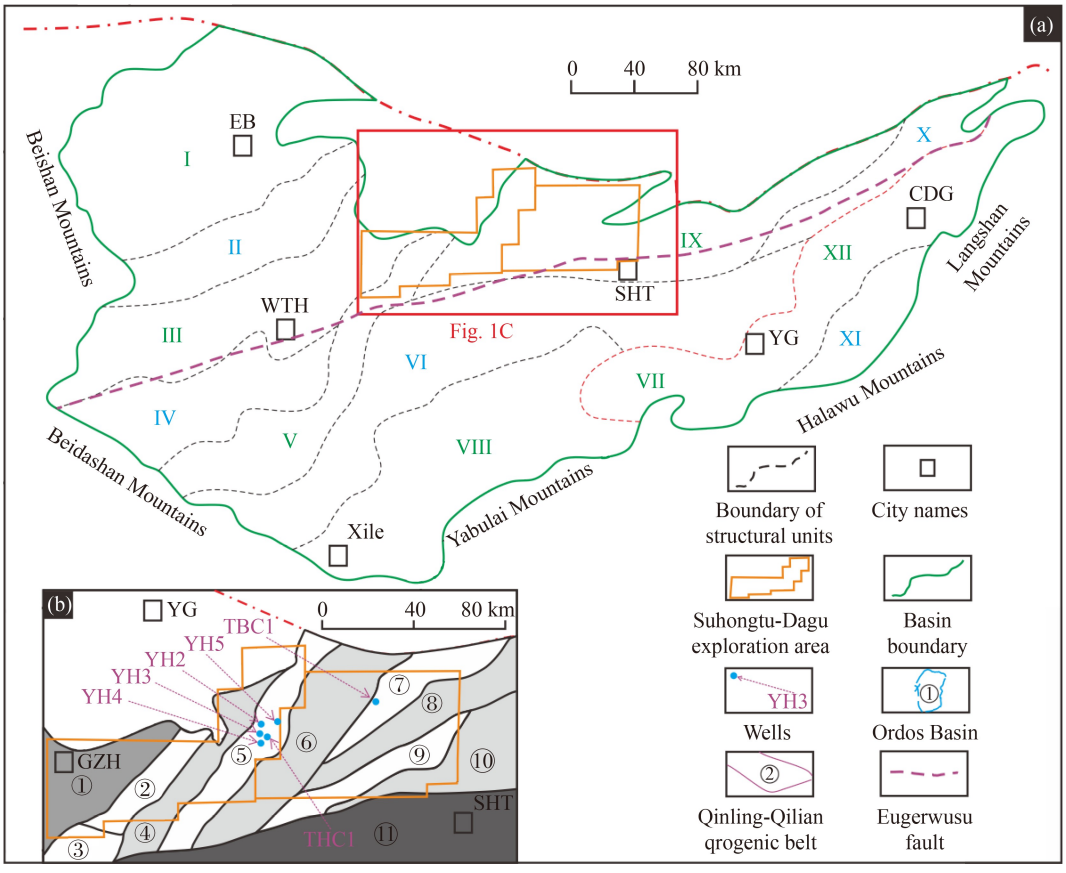

Fig. 1 (a) Yin'e Basin. I: Yanjuhai Depression, II: Lvyuan Uplift, III: Wutaohai Depression, IV: Teluoxitan Uplift, V: Dagu Depression, VI: Zongnaishan Uplift, VII: Shangdan Depression, VIII: Suhaitu Depression, IX: Suhongtu Depression, X: Chulu Uplift, XI: Benbatu Uplift, XII: Chagandelesu Depression. EB: Ejin Banner, WTH: Wutaohai, SHT: Suhongtu, YG: Yingen.CDG: Chadegan. (b) Research area. ① Guaizihu Slope, ② Guaizihu Sag, ③ Tukemu Sag, ④ Guaidong Swell, ⑤ Hari Sag, ⑥ Babula Swell, ⑦ Babei Sag, ⑧ Badong Swell, ⑨ Wulan Sag, ⑩ Aogao Swell, ⑪ Naishanchulu Uplift.

Table 1 Stratigraphy and seismic sequences of the Suhongtu-Dagu depressions

Erathem	Stratigraphic				Code	Tectonic Periods	Seismic Features	Seismic Sequences	Seismic Reflectance Interface
	System	Series	Formation	Member					
Cenozoic	Quaternary				Q	Himalayan	Downlap	A	T_Q
	Neogene								T_E
	Paleogene				R				
Mesozoic	Cretaceous	Upper	Wulansuhai		K_2w	Yanshanian	Onlap Truncation Downlap	B	T_{K2W}
			Yingen		K_1y			C	T_{K1Y}
		Lower	Suhongtu	Upper	K_1s_2			D	T_{K1S2}
				Lower	K_1s_1				
			Bayingebi	Upper	K_1b_2			E	T_{K1S1}
				Lower	K_1b_1				T_{K1B2}
Paleozoic	Permian				P	Hercynian	Truncation	F	T_G
	Carboniferous				C				T_P

thickness ranging from ~2 m to ~130 m with lithology of non-diagenetic brown and yellow conglomerate and gray mud conglomerate.

The Chagan Sag is a sub-structural unit in the Chagandelesu Depression in the north-east of the Yin'e Basin (Fig. 1), and is one of the oil-bearing depressions with the most exploration potential (Lu et al., 2017). The Suhongtu Depression located in the north-central part of the basin was a fault depression basin in the Mesozoic era and has a set of complex and diverse faults. Reservoirs

Table 2 Stratigraphic lithology in the Yin'e Basin

Formation				Lithology	paleontology
Cretaceous	Upper	Wulansuhai		Fine clastic sedimentary assemblage	Protoceratops sp., Bactrosaurus sp., Tyrannosauridae, Ankylosaurus
	Lower	Yin'gen		The mudstones are relatively concentrated, with the upper part dominated by gray mudstones, locally interbedded with siltstones and purplish-red mudstones; the lower part is a large suite of dark gray mudstones.	Laevigatosporites -Cicatricosisporites -Inaperturollenites
		Suhongtu	Su2	Relatively concentrated mudstone, the upper part dominated by gray mudstone and the lower part by large sets of gray calcareous mudstone	Classopollis-Piceaepollenites-Darwinula, ustella-Flabellochara hebeiensis, Classopollis-Piceaepollenites-Cicatricosisporites
			Su1	Relatively concentrated with dark gray mudstone in the upper part, brown and brown mudstone in the middle and lower parts, locally interbedded with dark gray mudstone	Concavissimisporites-Densoisporites-ClassopollisAtopocharatra-Chypeator jiuquanensis, Jiaohopollis-Palaeoconiferales-Cycadopites
		Bayingebi	Ba2	Grey sand conglomerate interbedded with calcareous siltstone in the upper part, dark gray calcareous mudstone interbedded with brown mudstone of unequal thickness in the middle, dark gray calcareous mudstone brown mudstone with brown-red mudstone interbedded with thinly bedded gray sand conglomerate of unequal thickness in the lower part	Protoconiferus, Classopollis, Cicatrieosisporites, Klukisporites, Cypridea unicostata
			Ba1	Large set of dark gray mudstones in the upper part, dark gray mudstones and brown mudstones in the middle, brownish red mudstones interbedded in unequal thickness, locally interbedded with calcareous siltstones, large set of dark gray and gray-black mudstones in the lower part	
	Carboniferous			Grey basalt and large suite of metamorphic conglomerates	
Permian				Volcanic, clastic and carbonate rocks of predominantly shallow marine phase	

have been found in the Lower Cretaceous, including the Bayingebi Formation, the Suhongtu Formation and the Yingen Formation in the Wuliji tectonic belt in the central tectonic belt (Lu et al., 2018; Chen et al., 2019c).

The Hari Sag is a sub-structural unit in the Suhongtu Depression in the north central part of the Yin'e Basin. The Bayingebi Formation of the Lower Cretaceous possessed a high yield of industrial oil flow. Drilling wells revealed that this set of strata contains oil-shale rocks and is rich in organic matters (Yang et al., 2017). It is a half-graven-like rift sag that had experienced fault-depression movements accompanied by continuous subsidence and formed a large set of mudstones containing abundant organic matters (Yang et al., 2017; Liu et al., 2019). Several lacustrine dark mudstones existed in the lower Cretaceous stratum, among which the source rocks of the Yingen Formation of micritic dolomite and dolomitic mudstone had the highest potential of hydrocarbon generation (Chen et al., 2017; Yang et al., 2017; Wang et al., 2019). Vitrinite reflectance (R_o) at the bottom of the Suhongtu Formation ranges from 0.6% to 1.2% while at the bottom of the Bayingebi Formation in the center of the sag is greater than 1.1% (Yang et al., 2017, 2018; Qi et al., 2018). Besides, the phenomenon that the Carboniferous-Permian system has a set of source rocks with large thickness, medium-high organic matter abundance, type II of kerogen in the majority, and moderate-high thermal evolution degree value indicates that the Permian strata have a good hydrocarbon generating potential (Lu et al., 2017, 2018). The Yhc1 well in the Hari Sag has multiple sets of intervals of natural gas shows. The reservoirs were the Yingen Formation of the Lower Cretaceous (Wei et al., 2014; Yang et al., 2018; Chen et al., 2019a), the Bayingebi Formation and the Permian Formations (Lu et al., 2018). Crude oil in the Bayingebi Formation came from the formation itself (Chen et al., 2019c), which has the possibility of self-generation and self-storage.

3 Data

Logging data from 11 drilling wells in the Hari Sag and the Babei Sag were collected, including wells of the Yhd1, the Yhc1, the Yhc2, the Yhc3, the Yhc4, the Yhc5, the Yhc6, the Ybd1, the Ybs1, the Yb1 and the Ybn 1 (Fig. 1).

A total of 2946 km of data from 64 2D seismic lines and 153 km^2 of 3D seismic data in the study area were collected, including data of the increased-density 2D seismic profile in the Hari Sag, a set of data from 4 seismic profiles, 3D seismic data which has wide frequency band and higher than 30−35 Hz of main frequency in the Hari Sag in 2016, as well as a set of data from 2D seismic profile of 1874.65 km in 2014. Except for the poor quality 2D seismic data in the desert area of the Guaizihu Sag, data of other seismic profiles are adequate for seismic inversion. The succession of seismic waves, well-identified structure and breakpoints can be interpreted.

4 Method

Comprehensive analysis of drilling and seismic data improves the accuracy of seismic interpretation in research. First, well-seismic calibration was conducted to identify the geological horizon represented by the seismic reflection. Second, based on the seismic coherence characteristics and 3-D visualization technology, the seismic horizons and faults were interpreted. Among them, the first step was to interpret the horizons and faults in the three seismic profiles passing through wells, then 3-D arbitrary well-connected profiles were created, and finally, the seismic volume in the entire area was determined and the spatial distributions of the seismic horizons and faults were obtained. Then, the seismic velocity spectrum data were corrected using the sonic data, and a velocity model was established by combining the seismic interpretation horizons and faults. Time-depth conversion was performed on the seismic interpretation horizons. Finally, the evolutionary history of the fault was investigated based on the results. The work flow of this research is illustrated in Fig. 2.

4.1 Horizon calibrations

The sequence stratigraphy adopted for this study is based on the division scheme of the Paleozoic Erathem and its overlapped strata in the Suhongtu area established by the Shaanxi Yanchang Petroleum Group in 2018 (Chen et al., 2019a).

Horizon calibrations were made by using the SynTool, a sub-module of the Landmark Workstation. Seismic waves of the Yingen Formation - the Bayingebi Formation in this area are clear and traceable regionally. The synthetic seismogram of the stratum featured as easy-traceable can be made using the ricker and statistical wavelets. After an environmental correction of acoustic and density curves of the 11 Wells, a series of synthetic seismic records of each well were made by convolution of the selected wavelet and logging reflection coefficient sequence. Later, the obtained time-depth results were input into the HRS software of reservoir prediction as initial conditions. The phase and amplitude spectrum of the seismic wavelets were decomposed from the seismic trace around the well and selected reasonable wavelet frequency and polarity to calibrate the horizon subtly. In this process, the correlation coefficient of the synthetic record and the seismic trace was used based on quality control. Logging geological stratification was adjusted according to the characteristics of the seismic interface, and the logging - seismic calibration was matched best.

4.2 Seismic horizon interpretation

Based on synthetic seismograms for 11 wells, the 2-D seismic profiles of 67 seismic lines with a total length of 2877 km and a 3-D seismic cube with a total area of 152 km^2 in the study area were interpreted, and the seismic horizons of K2w, K1y, K1s, K1b, P, and C were tracked.

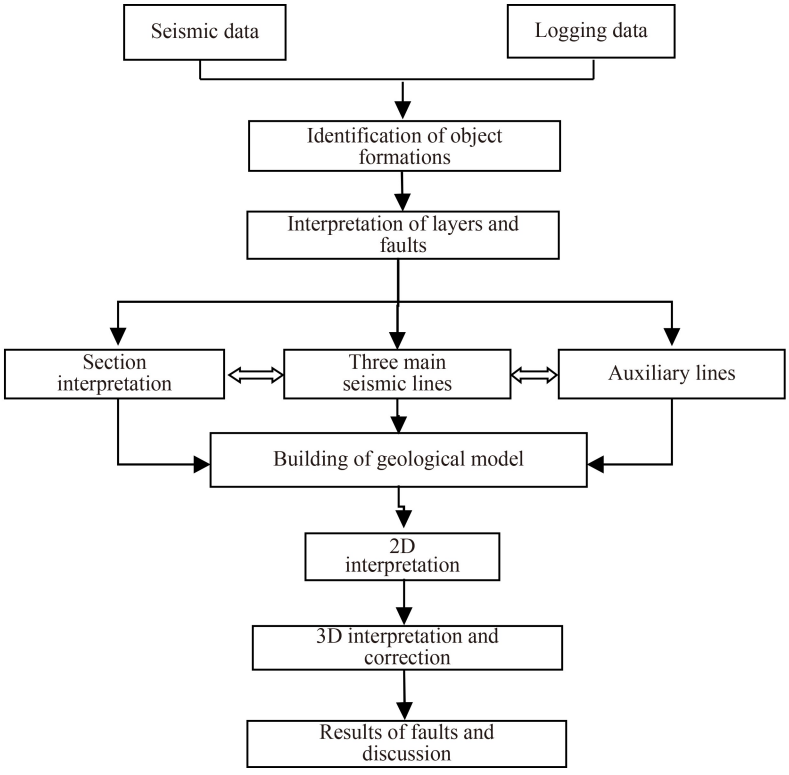

Fig. 2 Construction interpretation flow chart.

During the seismic interpretation, the main reflection target layers were determined by comparing the reflection characteristics and wave group relationships of each seismic horizon. Interpretation of an arbitrary connected well profile was carried out to determine the reflection characteristics of each target interval, and then, the analysis was expanded to the entire study area. The horizon closure of each polyline section was checked and modified until the horizon in the entire area was closed. Using a 3-D visualization technique, more accurate results were obtained based on the latest 3-D seismic data for the Hari Sag, and the unreasonable parts of the 2-D seismic interpretation were partially fine-tuned until the interpretation was accurate and reasonable throughout the entire area.

4.3 Fault interpretations

The basis for distinguishing faults on the seismic profile mainly includes the following seven points. 1) The reflected waves are staggered, bifurcated, merged, distorted, etc.; 2) the number of reflection events suddenly increases or decreases or disappears; 3) the wave group interval changes abruptly; 4) abrupt occurrence of reflection events or different reflection structures on both sides; 5) existence of section waves and diffraction waves; 6) small coordinated faults are generally developed near larger faults on the profile; 7) variation points of stratigraphic occurrence and inflection points in mostly suggest isolated small faults.

4.4 Establishment of velocity field and tectonic model

According to the drilling well velocity in the area, it is considered that there is little difference in wave velocity in the study area (Fig. 3). The time-depth gradient is relatively consistent with wells of the Ybc1, the Yhc1, the Ha1, and the Su1.

Burial depth of each set of strata in the study area was obtained by the time-depth conversion. The structural data of the reflection interface of each target layer in the study area were obtained after the correction of the floating datum level. Finally, the 3D seismic model of the Suhongtu-Dagu depressions was built (Fig. 4).

5 Results and interpretation

5.1 Horizon Tracking

The bottom boundary of the Yingen Formation can be identified in both logging curves and seismic profiles, which can be used as the marker layer of the whole area for stratigraphic tracking and comparison. Based on the corresponding relationship between seismic sequences and the geological stratification (Table 1), seven seismic sequences were interpreted, including the Permian System, the first and second members of the Bayinggebi Formation, the first and second members of the Suhongtu Formation, the Yingen Formation and the Wulansuhai Formation, with taking the synthetic seismogram of the well Yhc1 as an example (Fig. 5).

5.2 Seismic sequences

A case study of the Hari Sag shows the seismic sequence division (Fig. 6). The quality of seismic data collected in the Hari Sag is good with successive reflected wave-group in the target layer and easy-tracing of the wave group and the boundary reflection of the sag.

The bottom boundary of the Yingen Formation (K1y) is the unconformity contacting with the underlying formation. The phase of reflection is made by successive wave peaks. Seismic events showed a base lap in the sag, and the top cutting of the underlying reflector appears at the edge of the sag. The bottom boundary of the Suhongtu Formation (K1s1) is the parallel unconformity connected with the underlying layer. The reflector was made by successive wave troughs with a medium-weak-medium phase. Seismic events showed onlap at the edge of the sag and are parallel in the center of the sag. The bottom boundary of the Bayingebi Formation (K1b1) is the unconformity contacting with the underlying Paleozoic strata. The seismic reflection was characterized by 2–3 strong reflections that are not continuous. The lower reflection is truncated on the top.

All the boundaries mentioned above can be tracked across the entire area. The Permian – Carboniferous system was angularly contacted with its overlying strata. Seismic reflection was characterized by chaotic reflection and difficult to be traced across the entire area.

5.3 Fault interpretation results

Nearly 200 faults have been recognized by detailed interpretation of seismic data and all of them are normal faults, including 80 faults in the Hari Sag, 14 faults in the Babei Sag, 13 faults in the Wulan Sag, seven faults in the Guaizihu Sag and two faults in the Banan Sag, with taking the faults in the Hari Sag as an example (Table 3).

Faults are well-developed with a large quantity in the research area and all the interpreted faults are normal ones. Faults strike is inclined to the strata strike, which extends in the direction of NNE or NW. Faults in the study area can be divided several grades: Grade I faults, controlling structural belts, are the boundary lines of structural belts, with obvious cross-sectional characteristics and relatively large fault throws; Grade II faults control local structures, such as the two flank faults that form nose-shaped structures, the fault throw is not very large on the section, and the extension is short; Grade III faults, that is, those associated faults, small faults, etc. Faults of Grade-I controlled the foundation and sedimen-

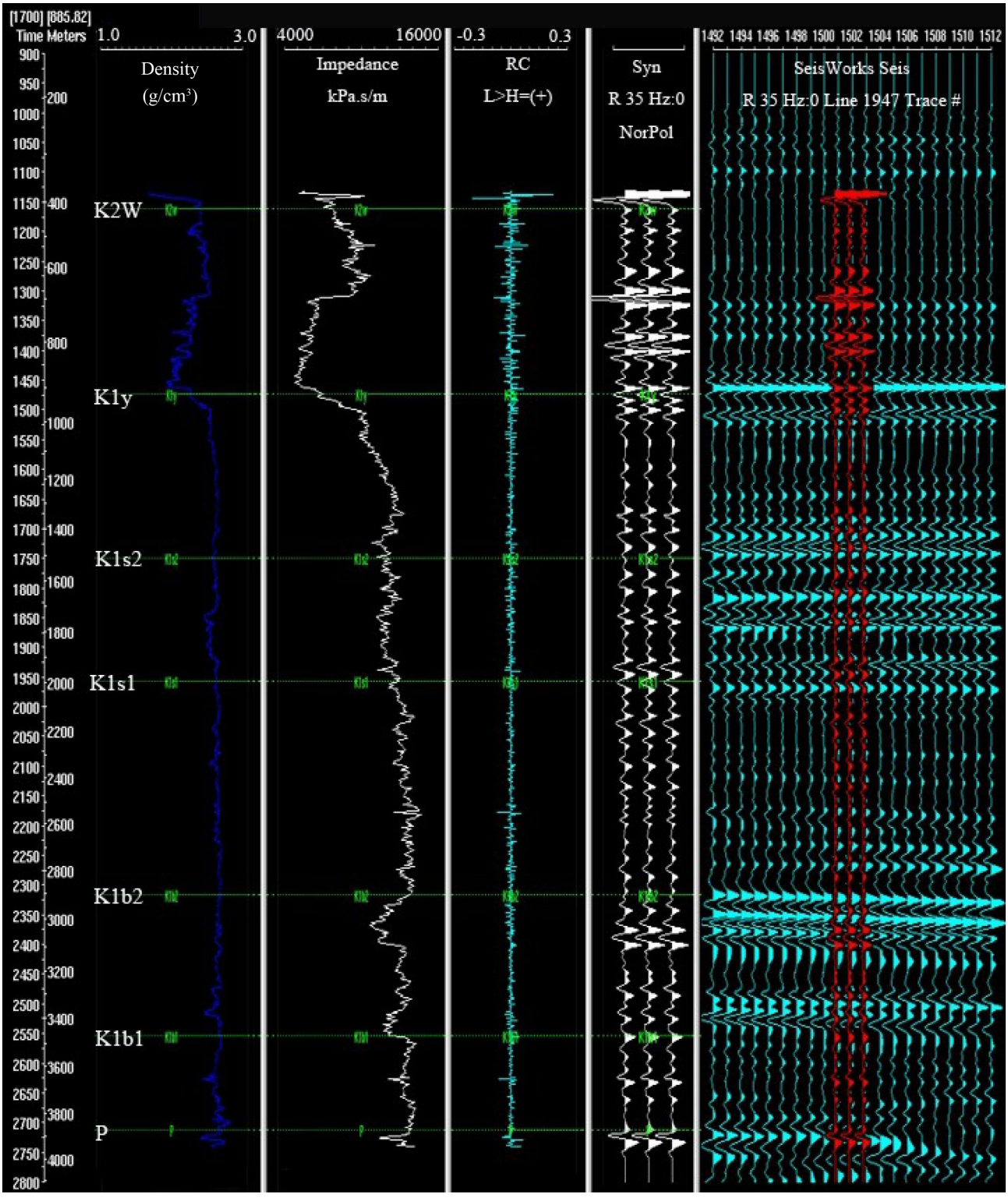

Fig. 3 Synthetic seismogram of the well Yhc1.

tary thickness of the Hari Sag, the Babei Sag, the Guaizihu Sag, the Wulan Sag and the Harinan Sag. Faults of Grade-II controlled the formation and development of local traps in the sags. The rests are small normal faults of Grade-III, which made the structure more complicated.

6 Discussion

The faults system of the Yin'e Basin is complex and varied, which manifests in fault strike, sequence and scale. The progressive deformation process of the inheritance faults and new faults was the reason leading

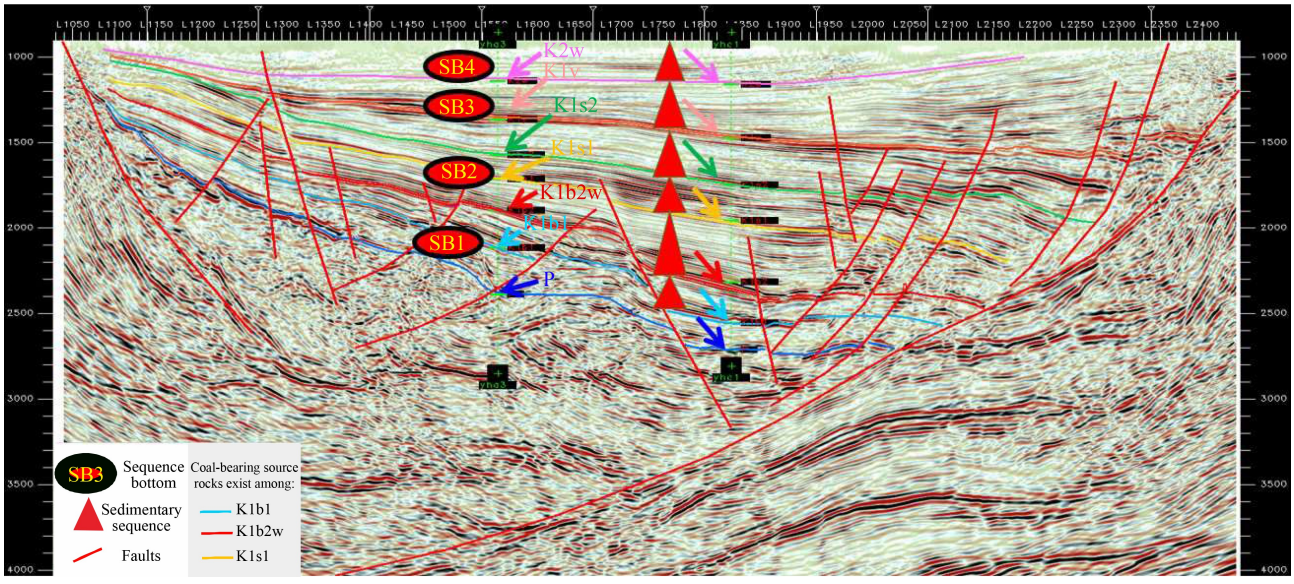

Fig. 4 Seismic line of YG14-199 passing the wells Yh3 and Yhc1.

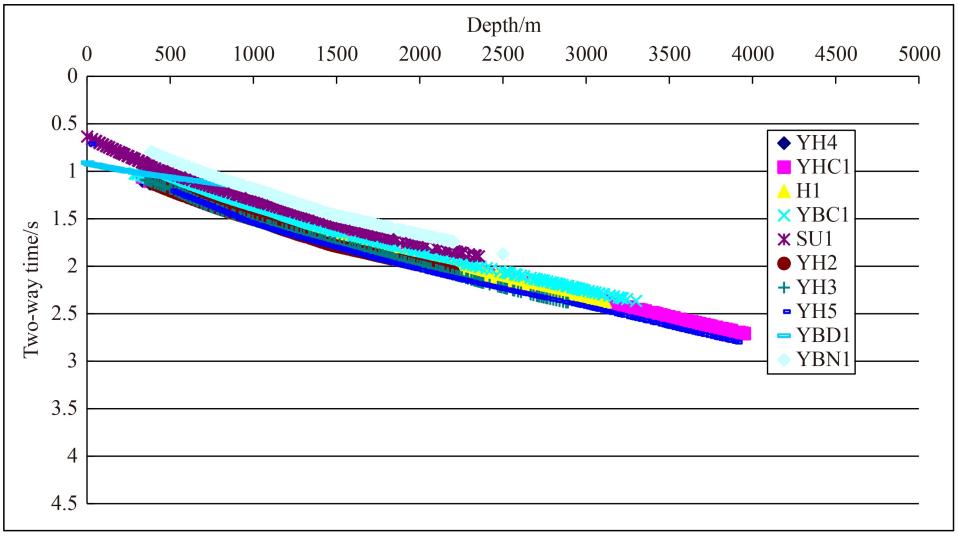

Fig. 5 Velocity analysis diagram of the exploratory wells.

to the formation of the complex fault systems (Lu et al., 2018; Wu et al., 2020a). The planar features, style and type, evolutionary stage as well as evolution mode of the Suhongtu-Dagu depressions are discussed comprehensively.

6.1 Planar features of faults in the SDD

Fault bottom boundary of the lower Bayingebi Formation, the upper Bayingebi Formation, the lower Suhontu Formation, the upper Suhongtu Formation, the Yingen Formation and the Wunansuhai Formation were calculated and the planar distribution maps were made. In general, the strike of the faults in the study area is mainly in the direction of NE or NNE. Major faults that have large displacement and extended widely played a role in controlling the boundaries of the Hari, Babei and Guaizihu sags.

In this study, we took the fault outlines of the K_1b_2 bottom boundary as an example (Fig. 7). These faults have the following features in planar geological maps. 1) The faults in the area developed in multiple stages, with relatively strong regularity. All the faults are normal ones striking NE and NNE, and the band characteristics on the plane are obvious. 2) The intensity and timing of fault activity in each sag are different. 3) The syn-sedimentary normal faults controlling the sag extend in the direction of NE and are distributed in an oblique pattern. Such faults have an early development period, a long active period, a large fault extension and a large fault throw. 4) Faults that control the secondary structural belt are mainly developed in the hanging wall of syngenetic faults in various sags.

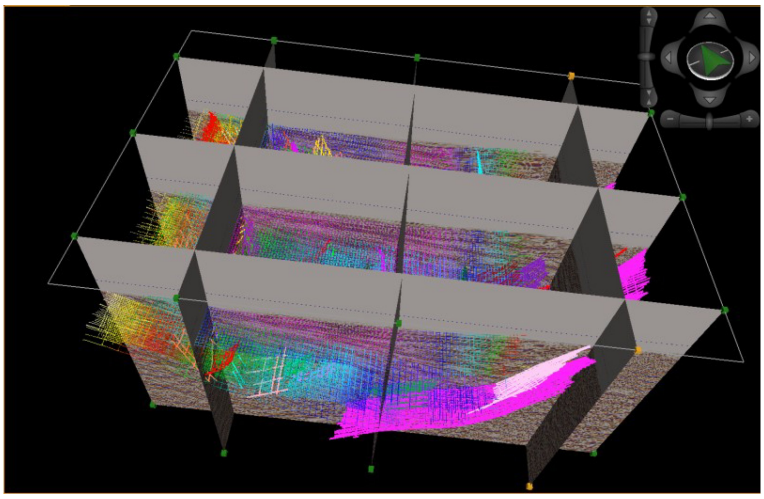

Fig. 6 3D seismic models of the Suhongtu-Dagu depressions. Lines in various colors are polygons of faults. The green arrow in the upper-left corner faces the north.

Table 3 Fault elements in the Hari Sag

Fault names	Extensional length/km					Displacement/m					Strike	Dip
	T_{k1y}	T_{k1s1}	T_{k1b}	T_p	T_c	T_{k1y}	T_{k1s1}	T_{k1b}	T_p	T_c		
hF1	37	42	44	45	51.4						NEE-NE	SSE-SE
hF2	22.2	22.4	21.8	22	13.2			400–1500	1200–2200	NE	SE	
hf1	26	27	27	28	30.4	50–600	50–600	50–800	100–800	500–2800	NE-NNE	SE-SEE
hf2	40	40	41	34	28.2	50–1200	200–2200	1000–2800	200–3000	1800–3000	NE-NNE	SE-SEE
hf3		6.4	6.2	4.8	3.8		200	50–200	10–180	100	NNE	SEE
hf4	17	16	15			50–100	50–100	200–400			NNE	SEE
hf5	24	24	15			50–100	200–600	400–700			NNE	SEE
hf6		12	12	11	10.4		100–200	50–200	20–400	200–600	NE-NNE	SE-SEE
hf7		6.2	5.8				50–100	50–200			NEE	SSE
hf8	11	11	10	9	4.6	100–200	200–600	50–600	200–600	220–600	NEE-NE	SSE-SE
hf9	8	9					50–200	400			NE	SE
hf10	12	7					50–100	50			NE	SE
hf11	7	12	12				50–100	50–200	50–200		NE	SE
hf12	18	18	17	6.4	6.2	10–100	200–600	50–200	50–100	50–100	NE	SE
hf13		7.6	12.2	13	13.2		50	50–100	200	200	NNE	SEE
hf14	25.6	25	21	19	18	10–50	50–100	100–200	20–400	50–400	NNE	SEE
hf15		6.4	6	3.6	3.2		100–200	100–200	20–200	10–50	NEE	SSE
hf16	7	6	5	5	4.6	100–200	50–200	50	50	50	NE	SE
hf17	9	6.6	6.4	6		50–100	50–100	50–100	100–200		NE	SE

Such faults have a relatively late development period and a short active period, and their main extension directions are NE, followed by NW, most of which are distributed in steps with sag-controlling faults. 5) Faults that are relatively developed in the direction of NE and with different lengths and complicatedly combined morphology include single row, parallel echelon, horsts and grabens.

6.2 Faults evolution history of sags

The evolution history of structural-faults of the Guaizihu Sag (② in Fig. 1(c)), the Hari Sag (⑤ in Fig. 1(c)) and the Babei Sag (⑦ in Fig. 1(c)) since the Cretaceous could be concluded based on the interpretation results of the section YG14-125, the section YG14-199 and the section YG243E (Fig. 8), which can be shown as follows.

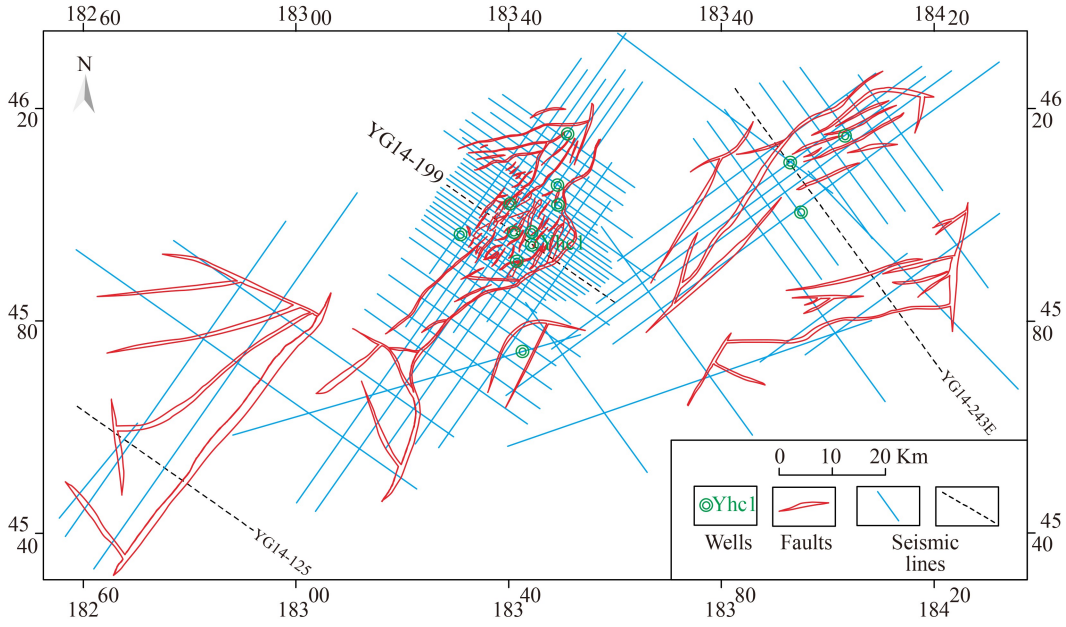

Fig. 7 Fault outlines of the K_1b_2 bottom boundary in the Suhongtu-Dagu depressions. Lines with blue and lines in black are all seismic lines, while the later ones are for tectonic interpretation in Fig. 8.

6.2.1 Evolution history of structural-faults in the Guaizihu Sag

The Guaizihu Sag underwent an uplift movement before the Cretaceous period, resulting in the loss of the Triassic-Jurassic strata and parts of the Carboniferous-Permian strata (Fig. 8). During the Cretaceous period, the basin resettled in the Cretaceous depositions. Under the action of extension, the half-graben - shaped fault depression in Guaizihu Depression was formed (Bai et al., 2018). After that, the regional left-lateral transtensional stress were strengthened, and the fault activities in the eastern boundary were intensified, which enhanced the differential subsidence amplitude of the Bayinggebi strata. During the sedimentary period of the Suhongtu Formation, the boundary faults continued to be active and the sag expanded significantly. During the sedimentary period of Yengen Formation, the effect of regional tensile stress field was enhanced, and the depression as a whole was settled differently, with the deposition thickening in the sag center. Later on, with the continuous uplift of the depression, the lake basin gradually disappeared to the end of Yingen Formation (Bai et al., 2018; Wu et al., 2020a).

6.2.2 Evolution history of the Hari Sag

In the Hari Sag, a regional uplift event accompanied by volcanic activity which happened before the Cretaceous period (Bai et al., 2018; Yang et al., 2018), caused the loss of the Triassic-Jurassic deposits and remained parts of Carboniferous-Permian strata after denudation (Fig. 8). In the Cretaceous, this region resettled and the Cretaceous strata were deposited. Under the tension and torsion stress of NW-SE were strengthened in the period of Bayinggebi Formation (Bai et al., 2018; Wu et al., 2020b), the half graben-like Hari Sag with a shape of steep in the east and gentle in the west was formed. General characteristics of the ancient topography at that time were high in the north and the west and low in the south and the east. Later on, the regional left-lateral tension and torsion stress were strengthened and the fault activities in the eastern boundary were intensified, enlarging the differential subsidence amplitude of the Bayinggebi Formation, and the volcanic activities continued during this period. During the Suhongtu sedimentary period, boundary faults remained active and volcanic rocks developed in the form of fissure eruption and the sag expanded. The tectonic evolution of Yingen Formation is similar to the Guaizihu Depression (Bai et al., 2018; Wu et al., 2020a).

6.2.3 Evolution history of the Babei Sag and the Wulan Sag

Like the Hari Sag, the Babei Sag had two tectonic stages with missing of the Triassic-Jurassic deposits (Fig. 8). Before the Cretaceous, the Permian-Carboniferous deposits in the Babei Sag were partial-residual, and during the sedimentary period of the Bayingobi deposition, the tectonic environment changed to extension. At the end of the sedimentary period of the Bayinggebi Formation, no deposits sedimented due to the regional uplift, and the sag was in the condition that fault in the west, overlapped in the east and thickened in the center. The Wulan sag began to develop the shape of a double-faulted sag both in the west and the east during the sedimentary period of the Bayinggebi Formation. Fault activities were more intense

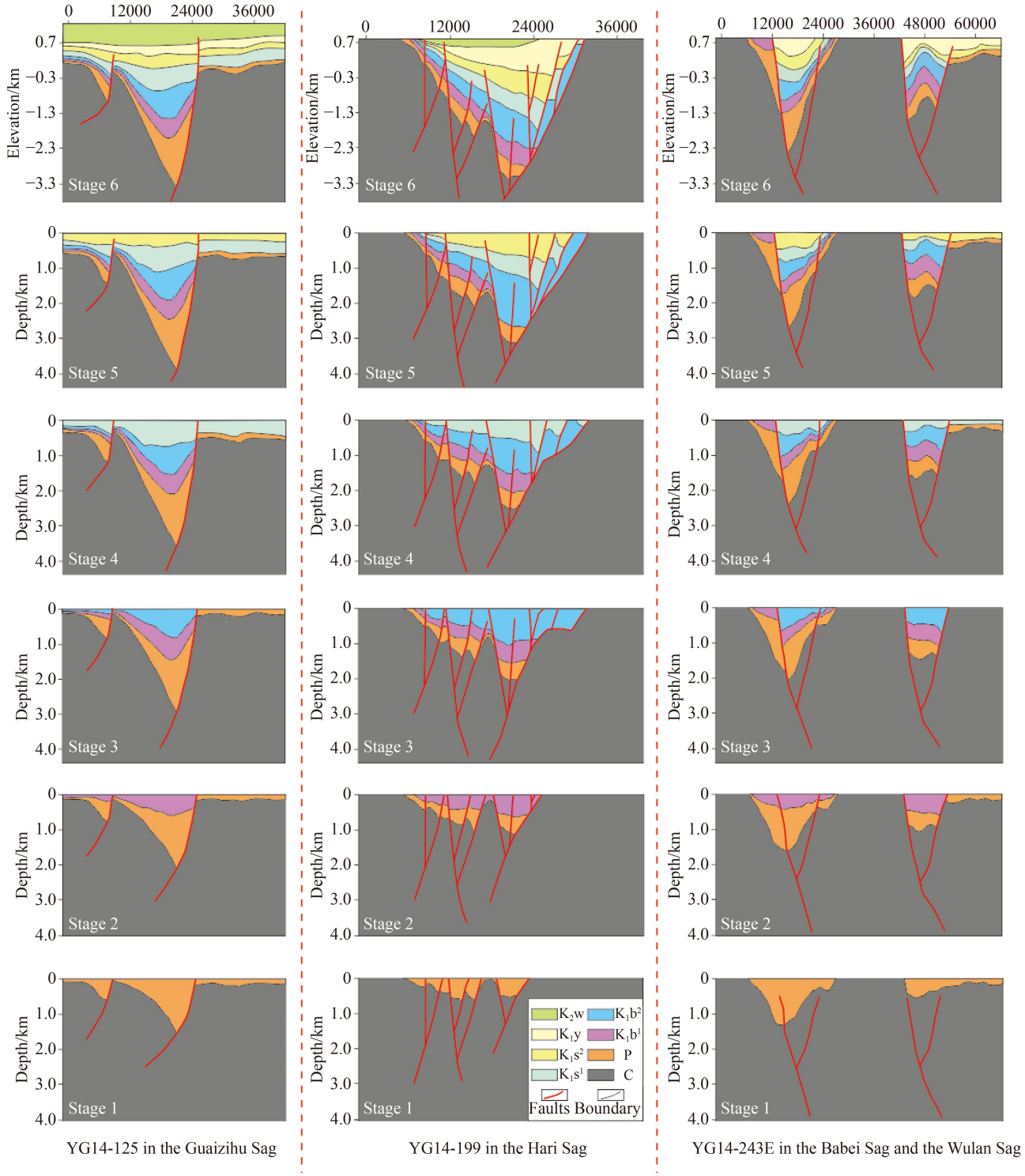

Fig. 8 Evolutionary history of faults in the Suhongtu-Dagu depressions. Stage1−Stage 6 refer to the moments before the deposits: the lower member of the Bayingebi Formation, the upper member of the Bayingebi Formation, the lower member of the Suhongtu Formation, the upper member of the Suhongtu Formation, the Yingen Formation and the Wulansuhai Formation, respectively. Locations of the YG14-125, the YG14-199, and the YG14-243E were shown in Fig. 7 as black dotted lines.

in the period of the Suhongtu Formation, which complicated the shape of the sag. Though both the Babei Sag and the Wulan Sag had a similar tectonic evolution with the Hari Sag, the thickness of the Cretaceous of these two formations was relatively small due to the weaker activities of the boundary faults at the deposition period of the Bayingebi Formation. The Bayingebi Formation, which was considered the best-evaluated source rock, has

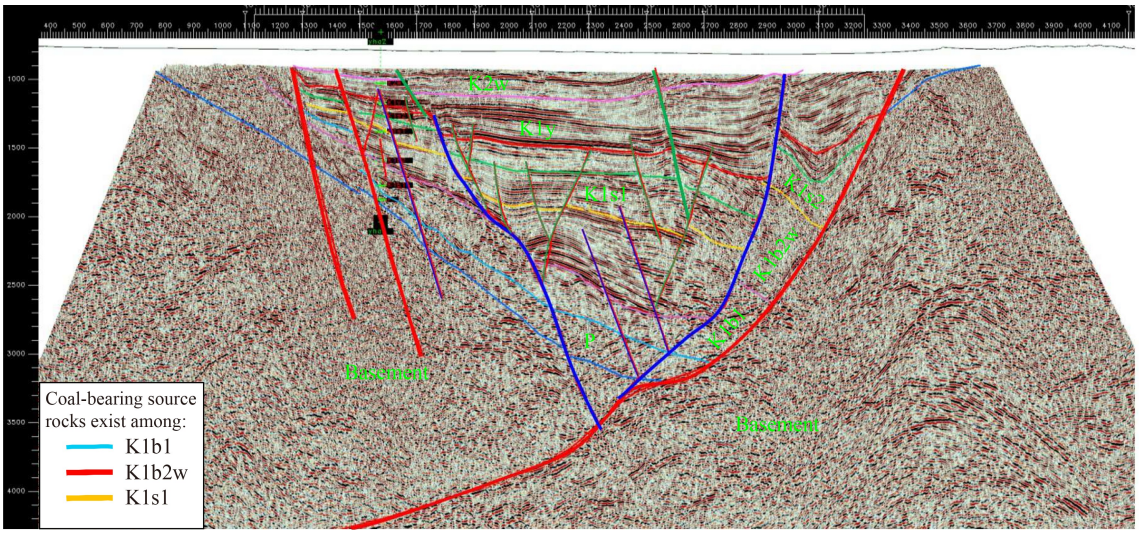

Fig. 9 Section characteristics of the faults. The lines in red, blue and green refer to the faults of Grade I, Grade II, and Grade III, respectively.

a relatively small sedimentary thickness. The evolutionary history of faults in the SDD indeed controlled the exploration potential of these sags.

6.3 Styles and types of faults in the SDD

The faults developed in this area included three main types on the seismic profile: 1) Y-shaped, 2) inverted-Y-shaped, and 3) parallel (Fig. 9). The type 1 faults are syngenetic faults that were developed during the Paleozoic and the Cenozoic. The type 2 faults occur from the top of the Permian to the Upper Cretaceous. The type 3 faults include some interstratified normal faults developed in the Cretaceous system (Fig. 9).

Since the Paleozoic, the successive fault development has shaped the basement of the area (red line in Fig. 9). Since the Late Permian, the formations have continued to uplift, resulting in the absence of Triassic strata in the depression. During the Jurassic, the regional structure inherited the tectonic features of the Late Permian uplift and denudation, and the sedimentary record of the Jurassic was lost until the depression was formed in the Cretaceous. In addition, the fault activity and sedimentary activity resulted in rift deposits. The seismic reflections in the Carboniferous and Cretaceous strata were interrupted or fractured in the seismic profile, forming a steep slope zone in the depressions. The dip angles of the faults are generally greater than 60°, and there are several small Y-shaped faults.

The faults from the top of the Permian to the upper Cretaceous are mainly the product of the overall stress response of the sag structure. The compressional stress state in the Late Jurassic gradually transformed into a tensional stress state. At this time, the sag faults began to develop under the influence of multiple regional volcanic events. Most of these faults cross the section from the top of the Permian to the top of the Suhongtu Formation or the Yingen Formation, and most of them are vertical normal faults. Although the interval between the faults is large, the sectional distance is generally medium to small, and most of the faults have large dip angles and are close to vertical. In the seismic section, obvious seismic in-phase axis dislocations can generally be observed, especially in the Bayangebi Formation and Suhongtu Formation. The faults generally do not extend very far, but they play a decisive role in the formation of the micro-structure and the hydrocarbon migration, accumulation, and trapping in the depression (Bai et al., 2018; Wu et al., 2020a).

Faults inside the Cretaceous stratum were small and formed by stress adjustment and accompanied by other faults. It is difficult to identify these faults in seismic profiles as they were generally developed inside the Bayingebi Formation and the Suhongtu Formation. Occasionally, some small “shook” seismic events in the section, which were isolated and difficult to develop continuously, had limited influence on traps and structures.

7 Evolutionary periods of faults in the SDD

The Yin’e Basin had undergone several tectonic events after the sedimentation of the Carboniferous – Permian System (Tian et al., 2016; Gillespie et al., 2017; Lu et al., 2017). Faults that occurred in each of the above evolutionary stages had various features. According to the formation and activity time, overlapping relationship with other faults and regional tectonic evolution, the progressive stages of faults were divided into three periods: 1) before the Early Cretaceous, 2) during the Early Cretaceous, and 3) post-Cretaceous.

7.1 Period I: before the Early Cretaceous

The syn-sedimentary faults, which were developed in the Devonian and ended in the Late Jurassic, contradicted with the development of the sags and controlled the sedimentation of five sags in the research area (red lines in Fig. 9). The faults that only passed across the basement were not sedimentary faults and formed in the end of the Late Jurassic with limited duration (Bai et al., 2018; Wu et al., 2020a).

These faults controlled the formation of the depression and the sedimentary deposites and they belong to the Grade-I of the SDD with features of an early beginning, longer displacement, longer duration, larger size.

Sag-boundary faults were formed with the evolution of the sags. These faults played a controlling role in the formation and development of the sags, but various roles in both the tectonic intensity and the thickness of the strata in each period. During the Mesozoic, the extensional subsidence in the Early Cretaceous was large and the effect on the structures and sedimentary construction of the depression was obvious. However, the activity intensity was different in the Early Cretaceous, showing that the activity intensity of the faults had the highest value in the Bayinggebi period, which decreased in the early stage of the Suhongtuo period, and increased in the late stage of the Suhongtuo period. This region entered the depression sedimentary period in the Late Cretaceous.

7.2 Period II: during the Early Cretaceous

Faults formed during the Early Cretaceous period were mainly developed in the interior of each sag and were located in the hanging wall of a large syn-sedimentary fault. Due to the regional extension, the subsidence rate of the hanging wall was accelerated during that period, resulting in the formation of a series of syngenetic normal faults. Most of these faults belong to the Grade-II faults of the SDD, which controlled the structural evolution of some areas. For example, the two wing faults that formed the nose structure had limited fault extension distance but controlled the distribution of tectonic belts (blue lines in Fig. 9).

The beginning deposition of the Bayingebi Formation was the time of the initial period of the depression. A series of secondary faults occurred in the interior of the depression at that time and disappeared with the stop of the deposition in the depression. The end of the Bayinggebi period was the end of the first sedimentary cycle in the depression, while the end of the Suhongtu was the time for the end of the fault depression with a low rise and tension of the depression. Furthermore, some faults were extension ones, while some were newly produced.

7.3 Period III: post-Early Cretaceous

Faults that formed after the Early Cretaceous were the latest phase ones in the study area and were caused by regional extension of the basin basement. The middle of each depression where the largest uplift amplitude of bedrock existed and was the place that faults developed intensively. Most of these faults belong to the third level of the SDD in Yin'e Basin, which are small in area, short in distance and extensive, accompanied by small dip angles and small scale graben structures (green lines in Fig. 9). At the end of the Early Cretaceous, a large-scaled tectonic movement with faults took place in this area, and the depressions were uplifted. The distribution of the coal seams of the Cretaceous Suhongtu Formation in the northern part of the Yin'e Basin was mainly controlled and influenced by the fault system during that period (Bai et al., 2018; Wu et al., 2020a).

8 Conclusions

Characteristics, evolution history and patterns of faults of the Suhongtu-Dagu depressions, the Yin'e Basin and their impact on coal seams in the Cretaceous System were made with the results as follows.

1) The faults of the SDD can be divided into three levels. The first is the syngenetic boundary faults which developed from Paleozoic to Cenozoic in each sag, the second is the faults located in each sag from the top of the Permian to the upper part of the Cretaceous, and the third is some interlayer adjusted normal faults developed in the Cretaceous strata. Different levels of faults with a certain inheritance controlled different sediments The faults are normal faults formed in multiple stages, which strike NEE and NNE in the plane and show three types of the "Y", the "anti-Y" and the "parallel" on the seismic porfiles.

2) Development of tectonics and sedimentations occurred at six main stages in the Hari Sag. The Guaizihu Sag and the Babei Sag, which were the main structural unit belts for oil and gas exploration in the north of the Yin'e Basin, had been largely controlled by the development and evolutionary history of the faults system since the Cretaceous.

3) Evolutionary periods of the faults in the SDD can be divided into the period I (before the Early Cretaceous), period II (during the Early Cretaceous), and period III (post-Early Cretaceous). Faults that formed before the Early Cretaceous and had been active since the Late Cretaceous, had the function of the controlling evolution of the depressions. The syn-sedimentary faults formed during the Early Cretaceous from the top of the Permian to the Upper Cretaceous and the reconstructive faults formed after the Early Cretaceous and developed in the Cretaceous System.

4) Faults in the SDD and the Yin'e Basin have the evolutionary patterns of controlling the formation of the depressions in the beginning. They controlled the sedimentation of sags, and finally slightly adjusted in the Cretaceous within the coal bearing strata. Distribution and evolution of the coal seams of the Cretaceous Suhongtu Formation were strongly controlled by the post-Cretaceous period, which is the third phase of fault evolution.

Acknowledgments We thank LetPub for its linguistic assistance during the preparation of this manuscript. This work is granted by the National Natural Science Foundation of China (Grant No. 42272152), the Major Projects from the Changqing Oilfield of PetroChina (No. ZDZX2021), the Fundamental Research Funds for the Central Universities, CHD (No. 300102272205), the Fundamental Research Funds for platform of Liangshan Characteristic Agriculture (015/500827), and the Innovation and Entrepreneurship Training Program for University Students, CHD (No. G202210710050).

References

Bai X Y, Han C C, He Y H, Ren L Y, Ma F X, Chen Z J, Liu H C (2018). Development characteristics of igneous rocks and its role in hydrocarbon accumulation in Hari Sag, Yingen-Ejinaqi Basin. Litho Reserv, 30(6): 18–26 (in Chinese)

Chen J P, He Z H, Wei Z B, Wang D L, Qin J Z, Guo J Y (2001). Geochemical characteristics of oil and source rock correlation in the Chagan Sag of Yingen-Ejinaqi Basin, NW China. Acta Sediment Sin, 19(2): 299–305 (in Chinese)

Chen Z J, Liu D, Liu H C, Ren L Y, Han W, Gao Y W, Zhao C C, Li K S (2018). Sedimentary characteristics and stratigraphic age of the thick-bedded coarse clastic rocks in the Yingen-Ejin Banner Basin, Northern China. Acta Sediment Sin, 36(3): 468–482 (in Chinese)

Chen Z J, Ma F X, Xiao G, Zhang Y, Gao Y W, Wang X D, Han C C (2019c). Oil-sources rock correlation of Bayingebi Formation in Hari sag, Yingen-Ejinaqi Basin. Oil Gas Geol, 40(4): 900–916

Chen Z J, Ren L Y, He Y H, Liu H C, Song J (2017). Geochemical characteristics and formation environment of high-quality hydrocarbon source rocks of Yingen Formation in Hari Sag, Yingen-Ejinaqi Basin. J Jilin U (Earth Sci Ed) , 47(5): 1352–1364 (in Chinese)

Chen Z J, Wen Z G, Liu H C, Zhang C M, Gao Y W, Bai X Y, Wang X D, Han C C, Li Z L, Li K S (2022). Geochemical characteristics and hydrocarbon generation potential of source rocks in Yihewusu Sag, Erlian Basin. J China U Petrol (Nat Sci Ed), 46(01): 34–43 (in Chinese)

Chen Z P, Ren Z L, Cui J P, Qi K, Zhang Y Y, Yu C Y, Ren W B, Yang G L, Liu R C (2019a). Age and petroleum geological implications of prolific formations in Hari Depression Well YHC1, Yin'e Basin. Oil Gas Geol, 40(2): 354–368

Chen Z P, Ren Z L, Qi K, Yu C Y, Ren W B (2019b). Zircon U-Pb chronology and geochemistry of volcanic rocks of early Cretaceous Bayingebi Formation in Suhongtu depression of the Ying'e Basin, and their tectonic implications. Acta Geol Sin, 93(2): 353–367

Fu G, Liang M G, Guo H Y, Han X, Li Q Q (2021). Prediction method of favorable positions of transporting oil and gas capacity configuration in different periods of faults. J Nat Gas Geosci, 6(2): 101–109

Gillespie J, Glorie S, Xiao W J, Zhang Z Y, Collins A S, Evans N, McInnes B, De Grave J (2017). Mesozoic reactivation of the Beishan, southern Central Asian Orogenic Belt: insights from low temperature thermochronology. Gondwana Res, 43: 107–122

Han W, Lu J C, Wei J S, Zhang Y P, Li Y H, Li Y (2015). Apatite fission track constraints on the Mesozoic tectonic activities in Shangdan Depression, Yin'e Basin, Inner Mongolia. Acta Geol Sin, 89(12): 2277–2285

Li J, Zhao C J, Liu G H, Zhang H, Zhang X, Ren K (2021a). Assessment of fault slip in shale formation during hydraulic fracturing and its influence factors. J China U Petrol (Nat Sci Ed), 45(02): 63–70 (in Chinese)

Li X, Jin L, Shen Z S, Sun D (2021b). Study on fault system evolution and low level faults characterization in the X Oilfield. Unconventional Oil & Gas, 8(05):19–26+44 (in Chinese)

Liu H C, Wang W H, Chen Z J, Zhao C C, Pan B F, Bai X Y (2019). Characteristics and accumulation conditions of Cretaceous dolomitic mudstone gas reservoir in Hari Sag, Yin'e Basin. Lithol Reserv, 31(2): 24–34 (in Chinese)

Liu X, Li T D, Geng S F, You G Q (2012). Geotectonic division of China and some related problems. Geol Bullet China, 31(7): 1024–1034 (in Chinese)

Lu J C, Song B, Niu Y Z, Wei X Y, Wei J S, Xu H H (2018). The age constraints on natural gas strata and its geological significance of Well Y in Hari Depression, Yingen-Ejin Basin. Geol Bullet China, 37(1): 93–99 (in Chinese)

Lu J C, Zhang H A, Niu Y Z, Liu H C, Chen Q T, Wei J S (2017). Carboniferous-Permian petroleum conditions and exploration breakthrough in the Yingen-Ejin Basin in Inner Mongolia. Geo China, 44(1): 13–32 (in Chinese)

Qi K, Ren Z L, Chen Z P, Cui J P (2021). Characteristics and controlling factors of lacustrine source rocks in the Lower Cretaceous, Suhongtu depression, Yin'e Basin, northern China. Mar Pet Geol, 127: 104943

Qi K, Ren Z L, Cui J P, Chen Z P, Ren W B (2018). Thermal history reconstruction of mesozoic source rocks in western of Suhongtu Depression, Inner Mongolia, northern China. Earth Sci, 43(6): 1957–1971 (in Chinese)

Ren Z L, Chen Z P (2020). Thermal Evolution History and Hydrocarbon Accumulation in Yingen-Ejinaqi Basin. Beijing: China Science Publishing & Media Ltd

Tian Z H, Xiao W J, Zhang Z Y, Lin X (2016). Fission-track constrains on superposed folding in the Beishan orogenic belt, southernmost Altaids. Geosci Front, 7(2): 181–196

Wang W, He D F, Gui B L (2017). Analysis of the structure feature and genetic mechanism of Manghan Fault Depression in south Songliao Basin. Unconventional Oil & Gas, 4(06): 19–25+63 (in Chinese)

Wang X D, Ren L Y, Liu H C, Chen Z J, Bai X Y, Zhao C C, Song J (2019). Characteristics and resource potential analysis of the Lower Cretaceous source rocks in the Hari Sag, Yin'gen-Ejinaqi Basin. J Xi'An U Sci Techn, 39(2): 286–293

Wei W, Zhu X M, Guo D B, Jiang F H, Tan M X, Wu C B J, Zhang J

F, Song J F (2014). Diagenesis and its controls on reservoir quality of Lower Cretaceous clastic rock reservoir in Chagan Depression of Yin-E Basin. Nat Gas Geosci, 25(12): 1933–1942

Wu X Z, He D F, Chen X M, Zheng M, Li Y Q (2020b). Geological characteristics and resource potential of the Yingen-Ejin Banner Basin. Chinese J Geo, 55(2): 404–419 (in Chinese)

Wu Z J, Han X Z, Lin Z X, Li Z N, Ji H, Yin D F, Jiang Z, Hu H (2020a). Tectonic, sedimentary, and climate evolution of meso-cenozoic basins in north China and its significance of coal accumulation and uranium mineralization. Geotectonica et Metallogenia, 44(4): 710–724 (in Chinese)

Xiao W J, Windley B F, Sun S, Li J L, Huang B C, Han C M, Yuan C, Sun M, Chen H L (2015). A tale of amalgamation of three Permo-Triassic collage systems in Central Asia: oroclines, sutures, and terminal accretion. Annu Rev Earth Planet Sci, 43(1): 477–507

Xing G Y, Qi K, Ren Z L, Cui J P, Zhang Y, Yang G L (2022). Diagenesis and hydrocarbon charging period in the Lower Cretaceous Bayingebi Formation, Hari sag, Yin'e Basin, northern China. Petrol Sci Techn, Published online: 11 Apr 2022

Yang P, Ren Z L, Xia B, Tian T, Zhang Y, Qi K, Ren W B (2018). Tectono-thermal evolution, hydrocarbon filling and accumulation phase of the Hari Sag, in the Yingge-Ejinaqi Basin, Inner Mongolia, northern China. Acta Geol Sin, 92(3): 1157–1169

Yang P, Ren Z L, Xia B, Zhao X Y, Tian T, Huang Q T, Yu S R (2017). The Lower Cretaceous source rocks geochemical characteristics and thermal evolution history in the HaRi Sag, Yin'e Basin. Petrol Sci Technol, 35(12): 1304–1313

Yin A, Rumelhart P E, Butler R, Cowgill E, Harrison T M, Foster D A, Ingersoll R V, Zhang Q, Zhou X Q, Wang X F, Hanson A, Raza A (2002). Tectonic history of the Altyn Tagh fault system in northern Tibet inferred from Cenozoic sedimentation. Geol Soc Am Bull, 114(10): 1257–1295

Yu Q, Ren Z L, Wang B J, Zheng W B, Tao N (2018). Geothermal field and deep thermal structure of the Tianshan-Altun region. Geol J, 53(S2): 237–251

Zhou Y S, Li H L, Shi D H, Chen F (2021). Characteristics of source rocks and enrichment laws of hydrocarbons in Yingen-Ejinaqi Basin. Acta Petrol Sin, 42(8): 1026–1038

AUTHOR BIOGRAPHIES

Qiang Yu, male, born in 1983 in Shaanxi Province, is currently an associate professor at the School of Earth Science and Resources, Chang'an University. His research interests focus on tectonothermal history recovery using thermochronology and geothermometry for petroleum accumulation and structural ore-forming model.
E-mail: yuqiang@chd.edu.cn.

Baojiang Wang, born in 1970 in Ningxia Province, is currently an associate professor at the School of Information Technology, Xichang University. His research interests focus on structural geology using seismic data and reservoir prediction for petroleum exploration.
E-mail: xcc20200168@xcc.edu.cn.

Zhanli Ren, born in 1961 in Shaanxi Province, is currently a professor at the Department of Geology, Northwest University. His research interests focus on tectonothermal history recovery and petroleum accumulation.
E-mail: renzhanl@nwu.edu.cn.

XianYao Sun, Xianghe Lei, Ahmed Khaled, and Qike Yang are all graduate students at the Chang'an University majoring in geology.